

Space- and time-like kaon electromagnetic form factors in perturbative QCD^{*}

JIN Dan(金丹)^{1;1)} YANG Ya-Dong(杨亚东)^{1;2;2)}

¹ Institute of Particle Physics, Huazhong Normal University, Wuhan 430079, China

² Key Laboratory of Quark & Lepton Physics, Ministry of Education, Wuhan 430079, China

Abstract: We present a phenomenological analysis of the space- and time-like charged kaon electromagnetic form factors in factorized perturbative QCD (pQCD) by employing an analytic model for $\alpha_s(Q^2)$ and an infrared (IR) finite gluon propagator. In the space-like region, due to the lack of available experimental data above $Q^2 \sim 0.2 \text{ GeV}^2$, we only give our results for intermediate energies and make no comparison. In the time-like region, our results agree reasonably well with the available experimental data at moderate energies, including the CLEO data and the J/ψ result.

Key words: electromagnetic form factor, perturbative QCD, analytical running coupling, twist-3 corrections, IR finite gluon propagator

PACS: 12.38.Bx, 12.39.St, 13.40.Gp **DOI:** 10.1088/1674-1137/36/10/004

1 Introduction

The electromagnetic form factors of hadrons provide useful information concerning the internal structures of the hadrons, and they also provide useful grounds to check the correctness of the perturbative QCD (pQCD) theory. During the past few decades, there have been extensive experimental and theoretical studies of pion electromagnetic form factors from various approaches. In comparison, there are fewer studies of kaon electromagnetic form factors. Experimentally, the kaon electromagnetic form factor in the space-like region is very poorly known and only measured at very low energies, as low as $Q^2 = -q^2 \leq 0.2 \text{ GeV}^2$ [1–4]. In the time-like region, there are more data up to several GeV^2 , however is suffers from very large uncertainties, a compilation of previously extracted kaon form factors for $Q^2 = q^2 < 10 \text{ GeV}^2$ is given in Ref. [5]. Theoretically, to our knowledge, there are very few theoretical efforts made for the kaon electromagnetic form factors, for example, the space-like kaon form factor has been studied in Refs. [6–12] based on different approaches. Following [12], the authors in Ref. [13]

present a combined investigation of the space- and time-like kaon electromagnetic form factors in light-cone perturbative QCD with transverse momentum dependence and Sudakov suppression. Since there is a total absence of experimental data for the space-like kaon form factor, and the precision of the existing time-like data is extremely poor, it is not possible to determine which approach describes the nature of the kaon form factor well. Recently, a high precision measurement of the kaon electromagnetic form factor has been made for a time-like momentum transfer of $Q^2 = 13.48 \text{ GeV}^2$ by the CLEO collaboration [14], and their result is: $Q^2 |F_K^{\text{tl}}(13.48 \text{ GeV}^2)| = 0.85 \pm 0.05(\text{stat}) \pm 0.02(\text{syst}) \text{ GeV}^2$, providing the first opportunity to critically test the theoretical predictions. Based on the phenomenological analysis of J/ψ decays, the time-like kaon form factor was estimated in Ref. [15] and the result is in excellent agreement with the CLEO data.

The purpose of this work is try to give a phenomenological study of the kaon form factors using the framework of perturbative factorization [16–18], in this way, we hope to give some meaningful predictions in the intermediate energy region. However, the

Received 20 January 2012, Revised 25 February 2012

^{*} Supported by National Natural Science Foundation of China (10735080, 11075059)

1) E-mail: jd2002@yahoo.cn

2) E-mail: yangyd@iopp.ccn.u.edu.cn

©2012 Chinese Physical Society and the Institute of High Energy Physics of the Chinese Academy of Sciences and the Institute of Modern Physics of the Chinese Academy of Sciences and IOP Publishing Ltd

Landau pole of the usual QCD running coupling tends to spoil the application of perturbative QCD (pQCD) at low and moderate momentum transfers. Hence, in this paper, we use an analytic prescription for the QCD running coupling (as proposed in Refs. [19, 20]) to eliminate the Landau pole. An important feature of such an analytic scheme is that it provides the possibility of simultaneously defining an analytical running coupling both in the space- and time-like region in a self-consistent way. In contradiction to the singular growth of the usual QCD running coupling in the infrared (IR) domain, the analytical running couplings have an IR fixed point, which is believed to enlarge the application of pQCD at low and intermediate energies and has been successfully applied to many hadronic processes, for example, to pion form factors [21–25].

The asymptotic pQCD prediction for the kaon electromagnetic form factors with only the twist-2 effects [18] completely fails to explain the currently available form factor data. In this paper, we emphasize the importance of including the twist-3 contribution to kaon form factors for obtaining good agreement with experimental data at moderate energies. In fact, the recent studies [11–13] show large twist-3 corrections to the kaon form factors, this is also confirmed in our analysis. However, the calculation of the twist-3 contribution always suffers from the endpoint divergence in collinear factorization approach. Hence, in our calculation of the hard scattering kernel, we will use the Cornwall [26] prescription of a gluon propagator with a dynamical mass to avoid enhancements in the soft end point. The use of this infrared (IR) finite gluon propagator is not only supported by the field theoretical studies [27–29], but also supported by the recent lattice QCD simulations [30].

2 Factorized pQCD

The approach for describing the kaon form factor is based on the so-called collinear factorization theorem [16–18] which is given by a convolution:

$$F_K^{\text{hard}}(Q^2) = \int_0^1 dx \int_0^1 dy \phi_K^{\text{in}}(x, \mu_F^2) \times T_H(x, y, Q^2, \mu_F^2, \mu_R^2) \phi_K^{\text{out}}(y, \mu_F^2), \quad (1)$$

where x and y are the longitudinal momentum fractions of the nearly on-shell valence quarks, μ_R is the re-normalization scale and μ_F is the factorization scale. The basic ingredients are: (a) a scattering ker-

nel T_H describing short-distance interactions at the parton level above μ_F and can be calculated perturbatively in the form of an expansion in the QCD running coupling, and (b) the kaon DA ϕ which encodes the long-distance information below μ_F and has to be determined by non-perturbative methods or extracted from relevant experimental data.

The dominant contributions to the kaon form factor come entirely from the leading Fock states, i.e., a $q\bar{q}$ valence quark configuration with interaction of one hard gluon between the two valence quarks. One of the four diagrams contributing to each of the Born amplitudes, $K\gamma^* \rightarrow K$ and $\gamma^* \rightarrow K^+K^-$, is shown in Fig. 1. The other diagrams correspond to allowing the gluon to interact on the other side of the photon vertex and allowing the photon also to couple to the other valence quark. The higher Fock state contributions are neglected, being suppressed by higher powers of $1/Q^2$.

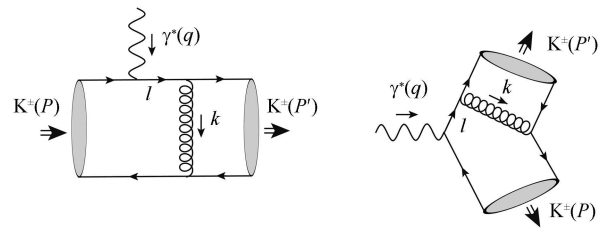


Fig. 1. Leading order Feynman diagrams in pQCD for hard contributions to the charged kaon electromagnetic form factors. Left: space-like region with $q^2 = (P' - P)^2 = t = -Q^2 < 0$. Right: time-like region with $q^2 = (P' + P)^2 = s = Q^2 > 0$.

To obtain the kaon form factors, we use the following light-cone projection operator of kaon in momentum space [31] (see Refs. [32–34] for a review):

$$\mathcal{M}_{\alpha\beta}^K = \frac{if_K}{4} \left(P \gamma_5 \phi_{2;K}(x, \mu) - \mu_K \gamma_5 \frac{k_2 k_1}{k_2 \cdot k_1} \phi_{3;K}^p(x, \mu) \right)_{\alpha\beta}, \quad (2)$$

where $f_K \approx 1.22 f_\pi \approx 160$ MeV [35] is the kaon decay constant defined by

$$\langle 0 | \bar{u}(0) \gamma_\mu \gamma_5 s(0) | K^-(P) \rangle = if_K P_\mu, \quad (3)$$

and $\mu_K \equiv M_K^2 / (m_u + m_s)$ is the chiral-enhancement parameter arising from the standard definitions of the twist-3 collinear DAs. k_1 and k_2 are respectively the quark and anti-quark momenta in kaon with momen-

tum P ,

$$k_1 = xP + k_\perp + \frac{\vec{k}_\perp^2}{2xP \cdot \bar{P}} \bar{P}, \quad (4)$$

$$k_2 = \bar{x}P - k_\perp + \frac{\vec{k}_\perp^2}{2\bar{x}P \cdot \bar{P}} \bar{P},$$

where x is the collinear momentum fraction carried by the individual valence quarks (x for the s quark and $\bar{x} \equiv 1 - x$ for the anti-quark \bar{u}), k_\perp is the transverse momentum of quark and anti-quark. \bar{P} is a light-like vector whose 3-components point into the opposite direction of \vec{P} , in this work, if we set P to be the initial kaon momentum, then \bar{P} corresponds to the final kaon momentum. As stressed in Ref. [34], the collinear approximation for the parton momentum (e.g. $k_1 = xP$ and $k_2 = \bar{x}P$) can be taken only after the light-cone projection has been applied.

$\phi_{2,K}(x, \mu)$ and $\phi_{3,K}^p(x, \mu)$ in Eq. (2) are the kaon twist-2 and twist-3 DAs, respectively. They can be derived from the light-cone QCD sum rules (LCSR) and are usually expressed as truncated conformal series expansion over Gegenbauer polynomials [36–38], e.g., the twist-2 DA is given by the following expression, in terms of Gegenbauer polynomials $C_n^{3/2}(2x-1)$:

$$\begin{aligned} \phi_{2,K}(x, \mu) &= 6x(1-x) \sum_{n=0,1,2}^{\infty} C_n^{3/2}(2x-1) \\ &\times a_n^K(\mu_0^2) \left(\frac{\alpha_s(\mu^2)}{\alpha_s(\mu_0^2)} \right)^{\gamma_n^{(0)}/\beta_0}, \end{aligned} \quad (5)$$

where α_s is the standard QCD running coupling, a_n^K are the Gegenbauer moments representing the non-perturbative inputs, $\gamma_n^{(0)}$ are the corresponding lowest order anomalous dimensions, and $\beta_0 = 11 - \frac{2}{3}n_f$ is the one-loop β -function coefficient. Note that the higher-order moments are extremely difficult to determine in their present determination. Hence, for practical calculations, the series expansion of the DAs is truncated only to the first few moments. In this paper, we adopt a model for the kaon twist-2 DA in truncating up to the second moment, as was done by Ball et al. in Ref. [38], the results at $\mu_0 = 1$ GeV are

$$\begin{aligned} a_1^K &= 0.06 \pm 0.03, \\ a_2^K &= 0.25 \pm 0.15. \end{aligned} \quad (6)$$

As for the twist-3 kaon DAs, in this paper, we neglect the 3-particle components. Furthermore, we use the asymptotic form, i.e.,

$$\phi_{3,K}^p(x) = 1 \quad (7)$$

for our analysis. The explicit formulas for the twist-

3 non-asymptotic collinear DAs can be found in Ref. [37].

Convolving the projection operator for the kaon DAs with the hard kernels using the factorization formula, (symbolically, $\mathcal{M}_{K;P'}^+ \otimes T_H^{LO} \otimes \mathcal{M}_{K;P}$), we have:

$$\begin{aligned} &(P' \pm P)_\mu \{F^{\text{sl}}, F^{\text{tl}}\}_K(Q^2) \\ &= \int_0^1 dx \int_0^1 dy \left(\frac{16\pi\alpha_s(k^2)e_f}{9} \right) \\ &\times \text{Tr} \left[\frac{\mathcal{M}_{K;P'}^+ \gamma_\alpha \not{l} \gamma_\mu \mathcal{M}_{K;P} \gamma^\alpha}{(l^2 + i\epsilon)(k^2 + i\epsilon)} \right. \\ &\left. + 3 \text{ other diagrams} \right], \end{aligned} \quad (8)$$

where e_f is the electric charge of the quarks, l and k are the internal quark and gluon momenta, respectively, as shown in Fig. 1. Computing the above equation carefully, we obtain the LO hard kernels:

$$\begin{aligned} \{T_H^{\text{sl}}, T_H^{\text{tl}}\}_K^{LO}(x, y, Q^2) &= \frac{8\pi f_K^2 \alpha_s(k^2)}{9} \\ &\times \left\{ \frac{\pm x Q^2}{(xQ^2 + i\epsilon)(xyQ^2 + i\epsilon)} \right. \\ &\left. + \frac{4\mu_K^2 x}{(xQ^2 + i\epsilon)(xyQ^2 + i\epsilon)} \right\}. \end{aligned} \quad (9)$$

As mentioned in the introduction, in this paper, in order to avoid the end-point divergence, we add two improvements into our calculations.

1) Firstly, we adopt the analytical running couplings [19, 20], which are believed to ensure the perturbative QCD calculation is reliable in the end-point region:

$$\alpha_s(k^2) \Rightarrow \{\alpha_s\}_{1,2}(k^2)$$

with

$$\{\alpha_s\}_1(k^2) = \frac{4\pi}{\beta_0} \left(\frac{1}{\ln(k^2/\Lambda^2)} + \frac{\Lambda^2}{\Lambda^2 - k^2} \right), \quad (10)$$

for the space-like region and

$$\{\alpha_s\}_2(k^2) = \frac{4\pi}{\beta_0} \left(\frac{1}{2} - \frac{1}{\pi} \arctan \left[\frac{\ln k^2/\Lambda^2}{\pi} \right] \right), \quad (11)$$

for the time-like region. Note that these analytical couplings freeze in the IR region: $\{\alpha_s\}_1(0) = \{\alpha_s\}_2(0) = 4\pi/\beta_0$ with the Landau pole being completely absent.

2) Secondly, we use the gluon propagator derived by Cornwall [26], to regulate the end-point divergent

integrals encountered within the pQCD formalism:

$$\frac{1}{k^2} \Rightarrow \frac{1}{k^2 - M_g^2(k^2) + i\epsilon},$$

where k is the gluon momentum. The dynamical gluon mass $M_g^2(k^2)$ is obtained as:

$$M_g^2(k^2) = m_g^2 \left[\frac{\ln(k^2 + 4m_g^2/\Lambda^2)}{\ln(4m_g^2/\Lambda^2)} \right]^{-12/11}, \quad (12)$$

where m_g is the effective gluon mass, with a typical value $m_g = 500 \pm 200$ MeV.

With the above two improvements, the LO hard kernels are then changed into:

$$\begin{aligned} & \{T_H^{sl}, T_H^{tl}\}_K^{LO}(x, y, Q^2) \\ &= \frac{8\pi f_K^2 \{\alpha_s\}_{1;2}(k^2)}{9} \\ & \times \left\{ \frac{\pm x Q^2}{(xQ^2 + i\epsilon)(xyQ^2 \pm M_g^2(k^2) + i\epsilon)} \right. \\ & \left. + \frac{4\mu_K^2 x}{(xQ^2 + i\epsilon)(xyQ^2 \pm M_g^2(k^2) + i\epsilon)} \right\}. \quad (13) \end{aligned}$$

After convolving the hard kernels with the kaon DAs, we obtain the final LO expresses up to twist-3 accuracy for the kaon electromagnetic form factors. Note that in this paper, we shall use the symbol F_K^{tl} for the time-like kaon form factor to distinguish it from the space-like counterpart F_K^{sl} :

$$\begin{aligned} & \{F_K^{sl}, F_K^{tl}\}_K^{LO}(Q^2) \\ &= \frac{8\pi f_K^2}{9Q^2} \int_0^1 dx \int_0^1 dy \{\alpha_s\}_{1;2}(k^2) \\ & \times \left\{ \frac{\pm 1}{xy \pm t^2 + i\epsilon} \phi_{2;K}(x) \phi_{2;K}(y) \right. \\ & \left. + \frac{4\mu_K^2}{Q^2} \frac{1}{xy \pm t^2 + i\epsilon} \phi_{3;K}^p(x) \phi_{3;K}^p(y) \right\}, \quad (14) \end{aligned}$$

where $\{\alpha_s\}_1(k^2)$ is defined by Eq. (10) and the $+$ signs correspond to the space-like case, while $\{\alpha_s\}_2(k^2)$ is defined by Eq. (11) and the $-$ signs correspond to the time-like case. The parameter $t^2 = \frac{M_g^2(k^2)}{Q^2}$ with the dynamical gluon mass $M_g^2(k^2)$ given in Eq. (12). It is observed that with respect to the space-like region, the integration in the above equation develops poles when $xy - t^2 + i\epsilon = 0$ in the time-like region. Thus, in general $|F_K^{tl}|$ should be larger than F_K^{sl} .

3 Numerical results and discussion

In this work, we calculate the factorizable hard contributions to the kaon form factors and give results at moderate momentum transfers. The behavior of $F_K(Q^2)$ at low momentum is dominated by the non-factorizable soft part. In Refs. [12, 13], the total charged kaon form factors can be written as $\{F_K^{sl}, F_K^{tl}\}(Q^2) = \{F_K^{sl}, F_K^{tl}\}^{\text{soft}}(Q^2) + \{F_K^{sl}, F_K^{tl}\}^{\text{hard}}(Q^2)$, to ensure a smooth matching of the different power-law Q^2 behavior between the soft and the hard parts, the authors introduce appropriate power correcting pre-factors to correct the hard parts in the low Q^2 region. This technique was originally done by Bakulev et al. in Ref. [25] for the pion form factor. Then the total form factors satisfied the Ward identity $\{F_K^{sl}, F_K^{tl}\}(Q^2 = 0) = 1$. In this work, we only plot the results at $Q^2 \geq 2$ GeV². In Refs. [36–38], the chiral parameter $\mu_K \approx 1.7$ GeV was used. However, in the context of the intermediate energies, μ_K is usually taken to be slightly lower ≈ 1.3 – 1.5 GeV. We therefore use $\mu_K = 1.5$ GeV for our analysis. Using the kaon DAs given in Eqs. (5), (6) and (7), we evaluated the kaon electromagnetic form factors Eq. (14) by varying the effective gluon mass from 0.3 to 0.7 GeV. Our final results are summarized in Fig. 2, along with the existing experimental kaon world data [1–5, 14] and the J/ψ result [15]. The solid, dashed-dotted and dashed lines represent $m_g = 0.3, 0.5$ and 0.7 GeV, respectively.

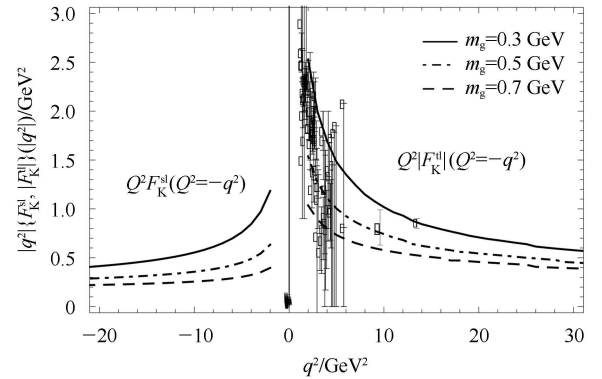


Fig. 2. PQCD predictions for the kaon electromagnetic form factors. The diamonds with error bars are the space-like world data [1–4], the solid points with error bars are the time-like world data [5], the box with error bar is the CLEO data [14] and the triangle with error bar is the J/ψ result [15] which is shown for comparison.

1) Space-like form factor: The space-like kaon form factor F_K^{sl} is shown in the left panel of Fig. 2. It is clear that the presently available kaon data in the space-like region are too limited and restricted only to the very low Q^2 region, below 0.2 GeV^2 . Due to this complete absence of the experimental data at intermediate energies, we are unable to make any meaningful phenomenological comparison. Hopefully, with the availability of better quality experimental data in the future, there could be a better testing ground for theoretical predictions.

2) Time-like form factor The time-like kaon form factor F_K^{tl} is displayed in the right panel of Fig. 2. In the time-like region, we plot the modulus of the kaon form factor since both the twist-2 and twist-3 corrections are complex. It is notable that the general enhancement of the time-like kaon form factor relative to the space-like one can be attributed to the time-like gluon propagator developing poles that are absent in the space-like region. Interestingly, it is found that the time-like kaon data below $Q^2 \sim 6 \text{ GeV}^2$ seem to reconcile reasonably with our predictions by choosing an appropriate gluon mass. Moreover, it is somewhat surprising to see that in combination with the twist-3 contributions, our predictions with $m_g = 0.3$ and 0.5 GeV show quite good agreement with the CLEO data [14] and the $J/\psi \rightarrow K^+K^-$ result [15]. However, whether such agreement is merely accidental is matter of debate. There may still be some theoretical uncertainties, e.g., from the chiral parameter μ_K , from the kaon DAs which are model dependent; the sub-leading contributions, e.g., from the NLO calculation in the strong running coupling, from the higher twists (e.g., twist-4, twist-5 or twist-6) or from the higher Fock state and the higher helicity components in the light-cone DAs. Moreover, the available data themselves have very poor statistics at intermediate energy and suffer from very large uncertainties. To this end, note that a full systematic theoretical NLO calculation for kaon form factors including the sub-leading twists is still missing. The higher helicity components' contributions to the kaon form factor are small in comparison with those of the usual helicity components [11]. The twist-4 contributions to the kaon form factor obtained in Ref. [13] are shown to be about a third of the magnitude of the twist-2 terms.

3) Twist-3 contributions The twist-2, twist-3 and the total contributions are summarized in Fig. 3. We fix the gluon mass $m_g = 0.3 \text{ GeV}$ and take both the space- and time-like kaon form factors for investigation. The dotted and dashed curves are twist-3 and twist-2 contributions, respectively, and the solid

curve is the sum. From Eq. (14), we can see the twist-2 contributions to the kaon form factors are suppressed by $1/Q^2$ and the twist-3 contributions are suppressed by $1/Q^4$, therefore, the twist-3 contributions are expected to be power suppressed in the high Q^2 region. However, in the low Q^2 region, the power suppression is not so tough and complemented by the chiral enhancement by a factor of $M_K/(m_s+m_d)$ and the large contributions near the end point since the twist-3 distribution function $\phi_{3;K}^p(x)$ does not fall off when $x \rightarrow 0,1$, so that the twist-3 contributions are found to be dominate in the low Q^2 region. Similar behavior can also be observed in the case with the $m_g = 0.5$ or 0.7 GeV , although we have not displayed them. As evident from the figure, the total scaled kaon time-like form factor up to twist-3 corrections displays an obvious improvement of the overall agreement with experimental data compared with the twist-2 scaled form factor. In this work, we neglect the 3-particle twist-3 DA, however, the contributions from the 3-particle twist-3 DA, being proportional to the non-perturbative parameter $f_{3K} \simeq 0.0045 \text{ GeV}^2$, are strongly suppressed by comparing with the 2-particle twist-3 DA parameter $\mu_K \simeq 1.5 \text{ GeV}$.

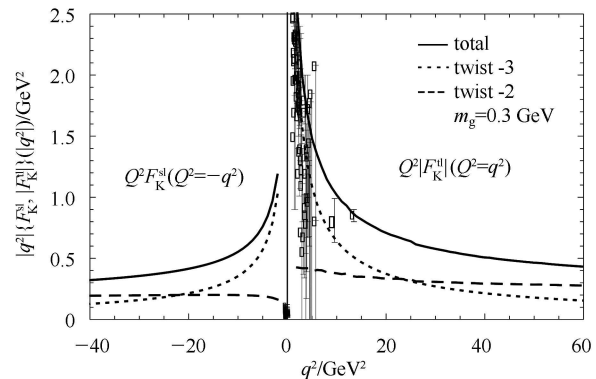


Fig. 3. The LO twist-2, twist-3 and total contributions to the kaon form factors. The solid, dotted and dashed curves are the total, twist-3 and twist-2 contributions, respectively.

4 Summary and conclusions

A precise knowledge of the meson form factor plays a key role in understanding the interplay between perturbative and non-perturbative physics at intermediate energies. In this paper, motivated by the recent CLEO data [14], we present a combined study on the kaon form factors for a broad Q^2 range by a combination of modeling and pQCD calculation. We have added two improvements: (a) replacing the

$\alpha_s(Q^2)$ by the analytic model, with the help of which, one can successfully enlarge the applicability of pQCD to the low and moderate range of energies, and (b) taking into account the power-suppressed twist-3 correction, which indeed helps explain the existing kaon data at experimentally accessible momentum transfers. However, when we calculate the twist-3 contributions, we meet the end-point divergence, hence, a non-perturbative gluon propagator

was adopted to prevent such enhancement in the end-point region. This Cornwall propagator involves a dynamical gluon mass $M_g^2(k^2)$ to regulate its infrared behavior. In summary, our predictions for the time-like kaon form factor are in good agreement with the available experimental kaon data, to be specific, the CLEO data [14] and J/ ψ result [15] can be well described by choosing the gluon mass $m_g = 0.3$ and 0.5 GeV, respectively.

References

- 1 Dally E B et al. Phys. Rev. Lett., 1980, **45**: 232
- 2 Amendolia S R et al. Phys. Lett. B, 1986, **178**: 435; 1986, **277**: 168
- 3 Zeidman B et al. CEBAF Experiment E91-016/1996
- 4 Niculescu G et al. Phys. Rev. Lett., 1998, **81**: 1805
- 5 Whalley M R. J. Phys. G, 2003, **29**: A1
- 6 Ji C R, Amiri F. Phys. Rev. D, 1990, **42**: 3748
- 7 Choi H M, Ji C R. Phys. Rev. D, 1998, **59**: 034001
- 8 XIAO B W, QIAN X. Eur. Phys. J. A, 2002, **15**: 523
- 9 Bijmans J, Khodjamirian A. Eur. Phys. J. C, 2002, **26**: 67
- 10 Pereira F P et al. Phys. Part. Nucl., 2005, **36**: 217
- 11 WU X G, HUANG T. J. High Energy Phys., 2008, **04**: 043
- 12 Raha U, Aste A. Phys. Rev. D, 2009, **79**: 034015
- 13 Raha U, Kohyama H. Phys. Rev. D, 2010, **82**: 114012
- 14 Pedlar T K et al. Phys. Rev. Lett., 2005, **95**: 261803
- 15 Kamal K S. Phys. Rev. D, 2007, **75**: 017301
- 16 Lepage G P, Brodsky S J. Phys. Rev. Lett., 1979, **43**: 545; Phys. Lett. B, 1979, **87**: 359; Phys. Rev. D, 1980, **22**: 2157
- 17 Efremov A V, Radyushkin A V. Phys. Lett. B, 1980, **94**: 245; Theor. Math. Phys., 1980, **42**: 97
- 18 Farrar G R, Jackson D R. Phys. Rev. Lett., 1979, **43**: 246
- 19 Shirkov D V, Solovtsov I L. Phys. Rev. Lett., 1997, **79**: 1209; JINR Rapid Commun., 1996, **2**: 5; Shirkov D V. Nucl. Phys. Proc. Suppl., 1998, **64**: 106
- 20 Milton K A, Solovtsov I L. Phys. Rev. D, 1997, **55**: 5295; Milton K A, Solovtsova O P. Phys. Rev. D, 1998, **57**: 5402
- 21 Stefanis N G, Schroers W, Kim H C. Phys. Lett. B, 1999, **449**: 299
- 22 Stefanis N G, Schroers W, Kim H C. Eur. Phys. J. C, 2000, **18**: 137
- 23 Karanikas A I, Stefanis N G. Phys. Lett. B, 2001, **504**: 225
- 24 Stefanis N G. Lect. Notes Phys., 2003, **616**: 153
- 25 Bakulev A P, Passek-Kumericki K, Schroers W, Stefanis N G. Phys. Rev. D, 2004, **70**: 033014
- 26 Cornwall J M. Phys. Rev. D, 1982, **26**: 1453; Cornwall J M, Papavassiliou J. Phys. Rev. D, 1989, **40**: 3474; Papavassiliou J, Cornwall J M. Phys. Rev. D, 1991, **44**: 1285
- 27 Aguilar A C, Natale A A, Rodrigues da Silva P S. Phys. Rev. Lett., 2003, **90**: 152001; Aguilar A C, Natale A A. J. High Energy Phys., 2004, **0408**: 057
- 28 Smekal L von, Hauck A, Alkofer R. Phys. Rev. Lett., 1997, **79**: 3591; Alkofer R, Smekal L von. Phys. Rept., 2001, **353**: 281; Fisher C S, Alkofer R. Phys. Rev. D, 2003, **67**: 094020; Alkofer R, Detmold W, Fisher C S, Maris P. Nucl. Phys. Proc. Suppl., 2005, **141**: 122
- 29 Zwanziger D. Phys. Rev. D, 2004, **69**: 016002; Howe D M, Maxwell C J. Phys. Lett. B, 2002, **541**: 129; Howe D M, Maxwell C J. Phys. Rev. D, 2004, **70**: 014002; Furui S, Nakajima H. AIP Conf. Proc., 2004, **717**: 685
- 30 Bogolubsky I L, Ilgenfritz E M, Muller Preussker M, Sternbeck A. arXiv: 0710.1968 [hep-lat]; Cucchieri A, Mendes T. arXiv: 0710.0412 [hep-lat]; Bowman P O et al. Phys. Rev. D, 2007, **76**: 094505 [hep-lat/0703022]
- 31 Geshkenbein B V, Terentev M V. Yad. Fiz., 1984, **40**: 758; Sov. J. Nucl. Phys., 1984, **40**: 487
- 32 Beneke M, Feldmann T. Nucl. Phys. B, 2001, **592**: 3
- 33 Beneke M, Nucl. Phys. B, 2002, **111**: 62
- 34 Beneke M, Neubert M. Nucl. Phys. B, 2003, **675**: 333
- 35 Chernyak V L, Zhitnitsky A R. Nucl. Phys. B, 1982, **201**: 492; Phys. Rep., 1984, **112**: 173
- 36 Braun V M, Filyanov I E. Z. Phys. C, 1989, **44**: 157; Z. Phys. C, 1990, **48**: 239
- 37 Ball P. J. High Energy Phys., 1999, **9901**: 010
- 38 Ball P, Braun V M, Lenz A. J. High Energy Phys., 2006, **0605**: 004